Inorganic Chemistry

Article

pubs.acs.org/IC

A Novel Diiminopyridine Ligand Containing Redox Active Co(III) Mixed Sandwich Complexes

Eleanor Magdzinski, Pierangelo Gobbo, Mark S. Workentin, and Paul J. Ragogna*

Department of Chemistry and The Centre for Advanced Materials and Biomaterials Research (CAMBR), The University of Western Ontario, 1151 Richmond Street, London, Ontario N6A 5B7, Canada

Supporting Information

ABSTRACT: The synthesis of a diiminopyridine (DIMPY) ligand containing pendant mixed sandwich cobaltocene functionalities on the imine nitrogens was prepared and characterized (**18**). Its reactivity with 2 equiv of $GeCl_2$·dioxane and $SnCl_2$ in THF yields the respective Lewis base mediated autoionization products (**18Ge** and **18Sn**). Analogous low-valent complexes utilizing an *N*,*N*′- differocenyl diiminopyridine support were also prepared (**15Ge** and **15Sn**). All compounds were characterized by spectroscopic and X-ray crystallographic methods. Electrochemical studies were conducted for both **15Sn** and the precursor of **18**.

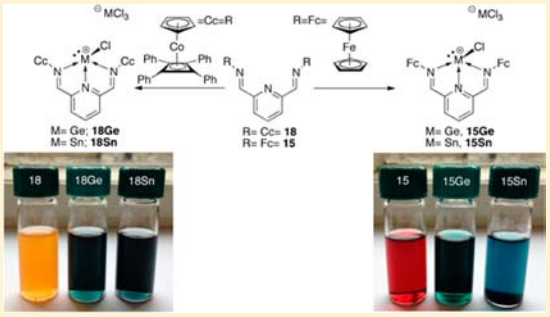

INTRODUCTION

Tunable catalysis by way of redox active ligands is a vast area with many different approaches for achieving control over a catalytic process.[1−6] Substitutionally inert redox-switchable ligands (or redox switches) are a category of ligand sets that form strong inert bonds to a given transition metal and are resistant to ligand exchange, as well as undergo controlled redox processes suitable for metal centered reactivity. These systems have recently shown promise as redox switches, where changes in the oxidation state of the ligand affect the reactivity of the metal by altering its electronic nature without changing its formal oxidation state (Scheme 1).[6]

Scheme 1. Schematic of Substitutionally Inert, Redox Active Ligands

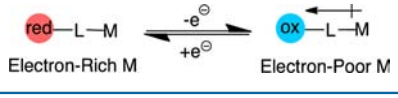

The redox activity originates from the incorporation of a functional group that can be readily oxidized/reduced reversibly either chemically or electrochemically and can include organic (e.g., hydroquinone,[7] naphthoquinone,[8] quinoxaline,[9] nicotinamide[10,11]) as well as organometallic substituents (i.e., ferrocene) onto an otherwise redox-inert ligand framework (Figure 1, **1**−**5**).

Ferrocene is often utilized as the redox active component because of its very well established electrochemical characteristics and for the stability of the sandwich complex in the oxidized and reduced states (Fe(II)/Fe(III)). Useful ligand frameworks that include ferrocene as an appendage are often nitrogen-based (Figure 2, **6**−**10**), where a few of these systems have proven to be useful for their ability to turn catalytically active complexes either 'on' or 'off' depending on the oxidation state of the ferrocene unit.[12−16]

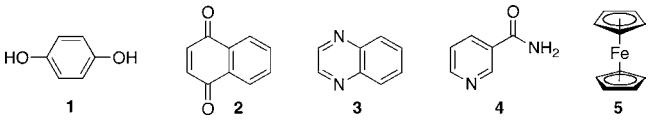

Figure 1. A few redox active moieties that have been used to impart redox activity onto substitutionally inert redox-switchable ligands.

A variety of other metallocenes have also been incorporated into redox active ligands to support transition metals, where the metallocene framework is affixed with pendant donor atoms. Aside from ferrocene, cobaltocene has been successfully employed as the redox active component (Figure 3, **11**−**14**);[17] Wrighton et al. synthesized a redox active 1,1′-bis(diphenylphosphino)cobaltocene ligand (Figure 3, **14**) capable of tunably controlling the rhodium(I)-catalyzed reduction and isomerization of ketones and alkenes by a ligand centered oxidation or reduction.[18,19]

The cobaltocene/cobaltocenium ligands (Figure 3, **11**−**13**) are found to be either formally neutral, 19 electron systems or cationic 18 electron complexes (Figure 3, **14**). The 19 electron cobaltocenes are highly reactive and readily oxidize to take on a more stable electronic conformation; however, the resulting 18 electron salts generally have poor solubility because of the cation−anion pair. These are complicating factors when attempting to both synthesize the ligands themselves and then utilize such fragments in subsequent chemistry. Therefore, to employ Co in such applications it would seem more favorable to construct a neutral, 18 electron complex, which

Received: June 24, 2013
Published: September 19, 2013

   dx.doi.org/10.1021/ic401598e | *Inorg. Chem.* 2013, 52, 11311−11319

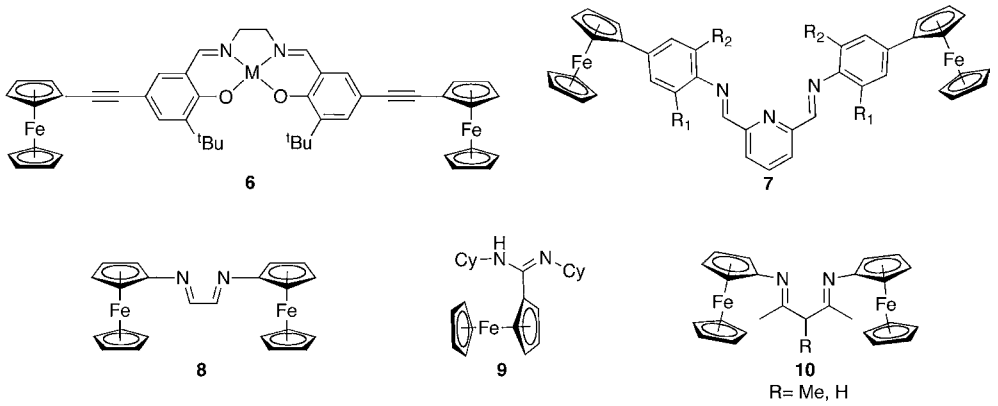

Figure 2. Select examples of nitrogen based ligands containing ferrocene.

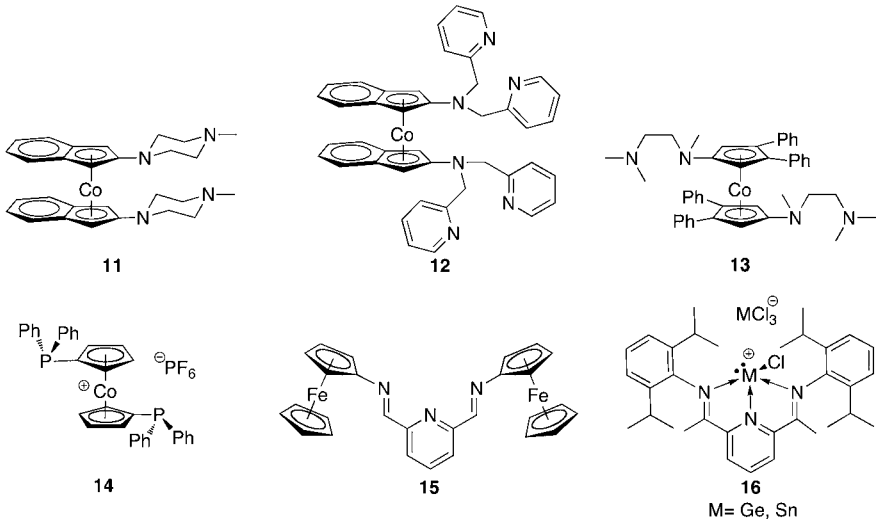

Figure 3. Ligands containing metallocene functionality (**11**−**15**) and a diiminopyridine ligand supporting tetrel (Ge, Sn) cations (**16**).

Scheme 2. Synthetic Route to 18

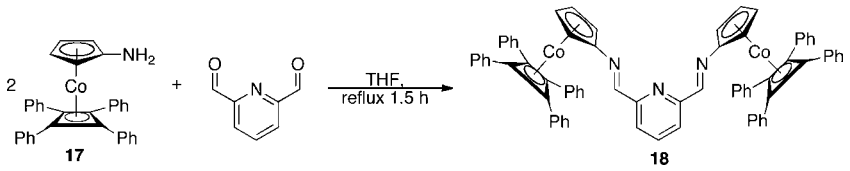

would enhance solubility, while maintaining stability.[20a−f] In this context, we now describe the synthesis of a novel diiminopyridine ligand containing mixed sandwich cobaltocene functionalites, unveil its reactivity with the tetrels (M = Ge, Sn), and comparatively discuss the electrochemistries of the free ligand and its *N*,*N*′,*N*″-M(II) chelates to their ferrocene analogues (Figure 3 for free ligand, **15**).[21,22]

RESULTS AND DISCUSSION

Compound **17**[20e] was reacted at reflux in THF with 2,6-pyridinedialdehyde in a 1:2 stoichiometry for 1.5 h, over which time the clear dark orange solution became opaque, bright orange. The slurry was then cooled to room temperature and centrifuged, and the resulting orange precipitate was washed. The volatiles were removed *in vacuo* yielding a bright orange solid that was sparingly soluble in all common organic solvents. A portion of the bulk solid was suspended in CD_2Cl_2, and a ^1H NMR spectrum was acquired. The insolubility of the compound made it difficult to assign peaks associated with the DIMPY framework; however a diagnostic downfield shift from cyclopentadienyl (Cp) protons (δ_H = 4.94 and 4.75 ppm) relative to the starting material (**17**; δ_H = 4.38 and 4.12 ppm) was apparent. High-resolution mass spectrometry was performed to further identify the product with a m/z = 1090.2972 corresponding to the expected m/z of a protonated DIMPY ligand containing pendant mixed sandwich cobaltocene functionalities (cf. 1090.2976). These results as well as those from the ^1H NMR spectrum led to the temporary assignment of the product as **18** (Scheme 2).

Compound **18** was then reacted with $GeCl_2$·dioxane at room temperature in a 1:2 stoichiometric ratio. The orange slurry immediately gave rise to a dark green-blue solution. After 1 h, the solvent was removed *in vacuo*, and the crude product was washed by adding a minimal amount of MeCN and then precipitating a green-black solid by the addition of Et_2O. A sample of the precipitate was redissolved in CD_2Cl_2 and the ^1H

dx.doi.org/10.1021/ic401598e | *Inorg. Chem.* 2013, 52, 11311−11319

NMR spectrum displayed downfield shifts for all protons relative to the free ligand and was consistent with findings for compound **18** binding to a metal center (Scheme 3, **18Ge**;

Scheme 3. Synthetic Routes to 15Ge, 15Sn, 18Ge, and 18Sn

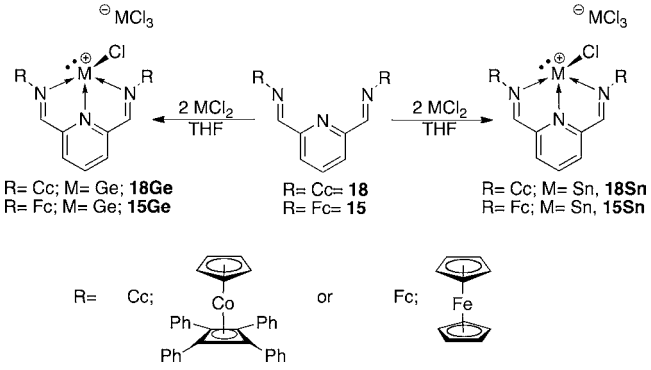

Table 1. ^{1}H NMR Chemical Shifts (ppm) for 15, 15Ge, and 15Sn in CD_3CN; 18Ge and 18Sn in CD_2Cl_2

	15	15Ge	15Sn	18Ge	18Sn
δ_H imine, 2H	8.81	9.13	9.18	7.56	7.64
δ_H *o*-py-d, 2H	8.21	8.21	8.17	7.80	7.72
δ_H *m*-py-t, 1H	7.84	8.56	8.52	8.64	8.59
δ_H H_α-m, 2H	4.71	5.21	5.13	5.10	5.26
δ_H H_β-m, 2H	4.35	4.83	4.79	5.33	4.99
δ_H H-Cp, 10H	4.21	4.39	4.42		
δ_H *o*-PhH-m, 16H				7.33	7.32
δ_H *p*-PhH-m, 8H				7.18	7.19
δ_H *m*-PhH-m, 16H				7.12	7.12

Table 1). A welcomed improvement in the solubility of this product relative to the sparingly soluble starting material was noted (Figure 4, middle). The cyclopentadienyl signals appear broad in comparison to the resonances of related systems and are likely a result of steric restrictions introduced by the formation of the *N*,*N*′,*N*″-chelated cationic Ge(II) center and an attenuation of the free rotation of the CbCoCp fragment. This is especially pronounced for Cp protons located on carbons β to the imine-nitrogen atoms, where the signal appears as a broad doublet (Figure 4, middle).

Compound **18** was then reacted with $SnCl_2$ at room temperature in a 1:2 stoichiometric ratio. After 12 h, the resulting dark brown-black slurry was centrifuged, and the eluent was decanted and dried *in vacuo* to yield a dark blue-black solid. A portion of the solid was redissolved in CD_2Cl_2, with a drastic improvement in solubility once again noted. The resulting ^{1}H NMR spectrum revealed diagnostic tin coupling for imine protons (δ_H = 7.68; $^3J_{Sn-H}$ = 32.0 Hz). Cyclopentadienyl protons β to imine nitrogens once again appear broad relative to those in similar systems. These findings, which agree with literature studies involving similar systems, led to the tentative assignment of the *N*,*N*′,*N*″-chelating cationic Sn(II) complex (Scheme 3, **18Sn**; Table 1).

In order to conduct a comparative electrochemical study, analogues of the group 14 complexes containing the previously reported *N*,*N*′-diferrocenyl diiminopyridine ligand (Figure 3, **15**) were prepared. The ligand (**15**) was treated separately with either $GeCl_2$·dioxane or $SnCl_2$ in a 1:2 stoichiometric ratio in THF at room temperature. After 5 min the initially red solutions turned dark green-blue. The solvent was removed *in vacuo* to yield a lustrous green or blue solid for Ge and Sn, respectively. Both compounds were redissolved in CD_3CN, and the ^{1}H NMR spectra displayed downfield shifts for all protons relative to the free ligand (Table 1). In both cases, signals associated with protons *para* to the nitrogen on the pyridine ring shift downfield relative to protons at the *meta*-position. A room temperature solution-state ^{119}Sn{^{1}H} NMR spectrum was also obtained for **15Sn**, consisting of two singlets (δ_{Sn} = −262.56 and −482.42), which are consistent with a cationic and an anionic Sn center, respectively (Supporting Information, Figure S-2).[22,23] These combined data led to the tentative assignment of the given solids as **15Ge** and **15Sn** (Scheme 3).

X-ray Crystallography. Suitable single crystals of **15Ge**, **15Sn**, **18Ge**, and **18Sn** were obtained by vapor diffusion of CH_2Cl_2 into hexane at 243 K (See Tables 2 and 3 for structures and Table 4 for X-ray data). Attempts to crystallize **18** by conventional techniques have thus far been met with failure due to the sparingly soluble nature of this compound. However, from the solid-state structures of **18Ge** and **18Sn**, any doubt to the identity of **18** is obviated. The molecular structures of all compounds reveal one cation consisting of a metal center (Sn or Ge) supported by a tridentate diiminopyridine ligand and one chlorine atom. The nature of the ligand for **18Ge** and **18Sn** successfully revealed the anticipated diiminopyridine framework containing pendant mixed sandwich cobaltocenes. Imine bond lengths were found to be consistent with those previously reported for diiminopyridine based frameworks (1.275(6) and 1.276(6) Å for **18Ge** and 1.274(3) and 1.280(3) Å for **18Sn**, cf. 1.26−1.29). The cation of all compounds adopts a distorted square pyramidal geometry. The deviation from planarity is more prominent in the Sn complexes (**15Sn** and **18Sn**), where the metal center prefers to lie below the ligand plane (−0.1577 Å for **18Ge**, −0.5275 Å for **18Sn**, −0.1577 Å for **15Ge**, and −0.3284 Å for **15Sn**). Even with this deviation, pyridyl nitrogens (N(2)) interact more strongly with main group centers than other nitrogens in the chelate (N(2) and N(3)). In all cases, the bound chlorine atom is oriented perpendicular to the ligand framework. Each cation is paired with a trigonal pyramidal MCl_3^- anion (M = Sn or Ge) The bonding arrangements of these compounds show little deviation from those previously reported by Roesky and co-workers who initially investigated the formation of such complexes utilizing a 2,6-diacetylpyridinebis(2,6-diisopropylanil) ligand support (see Figure 3, **16**, for structures; Table 5 for salient bond lengths and angles for comparison, **16Ge** and **16Sn**). Other than **18Ge**, all metallocene substituents prefer to rest *syn* relative to the diiminopyridine framework. This can be explained upon examining the N−M(1)−Cl(1) bond angles. In the case of **18Ge**, the N(1)−M(1)−Cl(1) is much less than in the other compounds, causing the Cl(1) atom to lean slightly toward the N(1) side of the molecule, resulting in the mixed sandwich on N(1) to lie *anti* to the ligand plane. It is interesting to note that the Cp rings bound directly to imine nitrogens are found out of plane with respect to the ligand basal plane. This is unusual, because past examples depict the Cp rings lying preferentially in a conjugated linear plane alongside of the diiminopyridine framework, but can be explained by the addition steric restrictions posed by the Cl(1) atom.

Electrochemistry. The cyclic voltammogram of the ligand precursor, **17**, was recorded in CH_2Cl_2/0.1 M $TBAPF_6$ using a Pt disk electrode as the working electrode (Figure 5). The CV

dx.doi.org/10.1021/ic401598e | *Inorg. Chem.* 2013, 52, 11311−11319

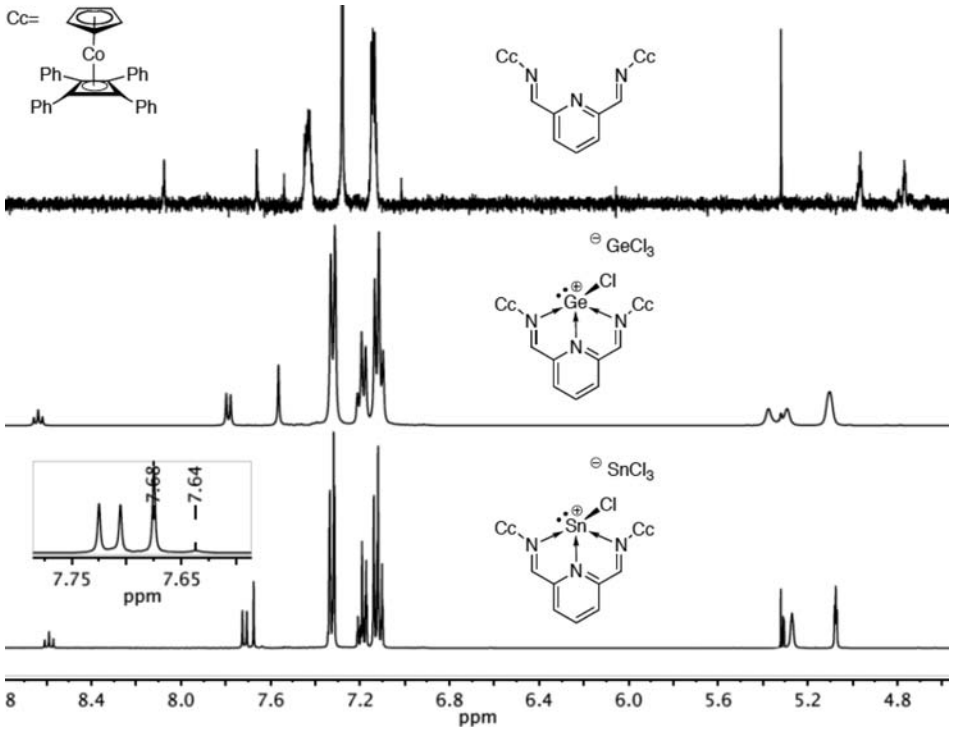

Figure 4. ^{1}H NMR spectra for compounds **18**, **18Ge**, and **18Sn** from top to bottom in CD_2Cl_2 on a 400 MHz spectrometer showing an increase in solubility from free ligand (**18**) to Ge (**18Ge**) and Sn (**18Sn**) complexes. Inset, imine protons on **18Sn** at δ_H = 7.68. Proton NMR spectra for **18Sn** were obtained at 400 and 600 MHz to confirm the presence of ^{119}Sn satellites (400 MHz δ_H = 7.64).

exhibits a two-electron, chemically reversible oxidation peak potential of 0.98 V and with E^0 = 0.87 V vs the quasi Ag/AgCl reference electrode. The peak is chemically reversible at scan rates higher than 1 V s^{-1}, while at lower scan rates, it was irreversible. The internal standard, nitrobenzene, has an E^0 = −0.90 V under the identical conditions. For **17**, in cases where the potential vertex was more positive than 1.45 V, additional oxidations occur, and the oxidized species decomposes at potentials higher than 1.45 V (also shown in Figure 5). Unfortunately, it was not possible to characterize compounds **18**, **18Ge**, and **18Sn** because they were poorly soluble at appropriate concentrations and the compounds were found to be electrochemically unstable giving irreproducible results because the products lead to electrode fouling, although features expected for the Co oxidation were evident.

The corresponding ferrocene derivative **15Sn** was characterized by cyclic voltammetry (CV). In this case, the electrochemical experiment was carried out in 5 mL of MeCN/0.1 M $TBAPF_6$ electrolyte solution and a GC disk was used as the working electrode. The CV of **15Sn** recorded at 0.5 V s^{-1} of scan rate (Figure 6) shows a one-electron chemically reversible peak at −0.46 V with a standard potential of E^0 = −0.43 V (internal standard, nitrobenzene reduction E^0 = −1.05 V) that is most likely related to a reduction about the cationic metal center. This signal is absent in the CV of the ligand **15**.[21] The CV also shows an apparent two-electron, chemically reversible peak at 1.03 V that is related to the consecutive oxidation of the two ferrocene moieties belonging to the DIMPY ligand at very similar oxidation potentials. Upon change of the electrolyte from $TBAPF_6$ to tetraoctyl phosphonium tetrakis(pentafluorophenyl)borate ($P_{8888}TB$), the two overlapping oxidation peaks of the two ferrocene moieties are distinguishable with oxidation peaks at 0.88 and 0.96 V at 0.1 V s^{-1}, respectively (Figure 7). This is in line with what was previously observed with other low valent main group complexes supported by an *N,N′*-differocenyl diiminopyridine framework.[21] The CV characterization of the other FcDIMPY complexes was not possible. These complexes also have very poor solubility in suitable solvents and lead to poorly resolved and irreproducible voltammograms due to electrogeneraterd decomposition at the electrode surface under these conditions.

■ CONCLUSIONS

A bulky diiminopyridine ligand containing mixed sandwich cobaltocenes (**18**) was prepared. Reactivity of **18** with 2 equiv of $SnCl_2$ and $GeCl_2$·dioxane lead to the formation of the respective low valent cation−anion pair (**18Ge** and **18Sn**). The cation is supported by the *N,N,N″*-DIMPY chelate as well as one chlorine atom and takes on a distorted square pyramidal geometry. The anion adopts a pseudo-trigonal-pyramidal geometry with three chlorine atoms oriented about the main group center. Main group analogues utilizing the *N,N′*-differocenyl diiminopyridine ligand were also synthesized (**15Ge** and **15Sn**). Although the majority of the compounds displayed instability to the electrochemical conditions employed, the amine precursor of **18** (Scheme 2, **17**) and **15Sn** were studied. Investigations of **15Sn** in MeCN/0.1 M $TBAPF_6$ show two events: a one-electron chemically reversible peak at −0.46 V with a standard potential of E^0 = −0.43 V and a two-electron chemically reversible peak in the oxidation at 1.03 V due to the consecutive oxidation of the two ferrocenyl moieties at similar potentials. Changing the electrolyte from $TBAPF_6$ to tetraoctyl phosphonium tetrakis(pentafluorophenyl)borate ($P_{8888}TB$) allows us to better distinguish the two overlapping peaks of the ferrocenes. Compound **17** shows a reversible two-electron oxidation peak at 0.98 V and with E^0 = 0.87 V. This result supports the possibility for harnessing the redox activity

dx.doi.org/10.1021/ic401598e | *Inorg. Chem.* 2013, 52, 11311−11319

Table 2. Solid-State Structures of 18Ge and 18Sn[a]

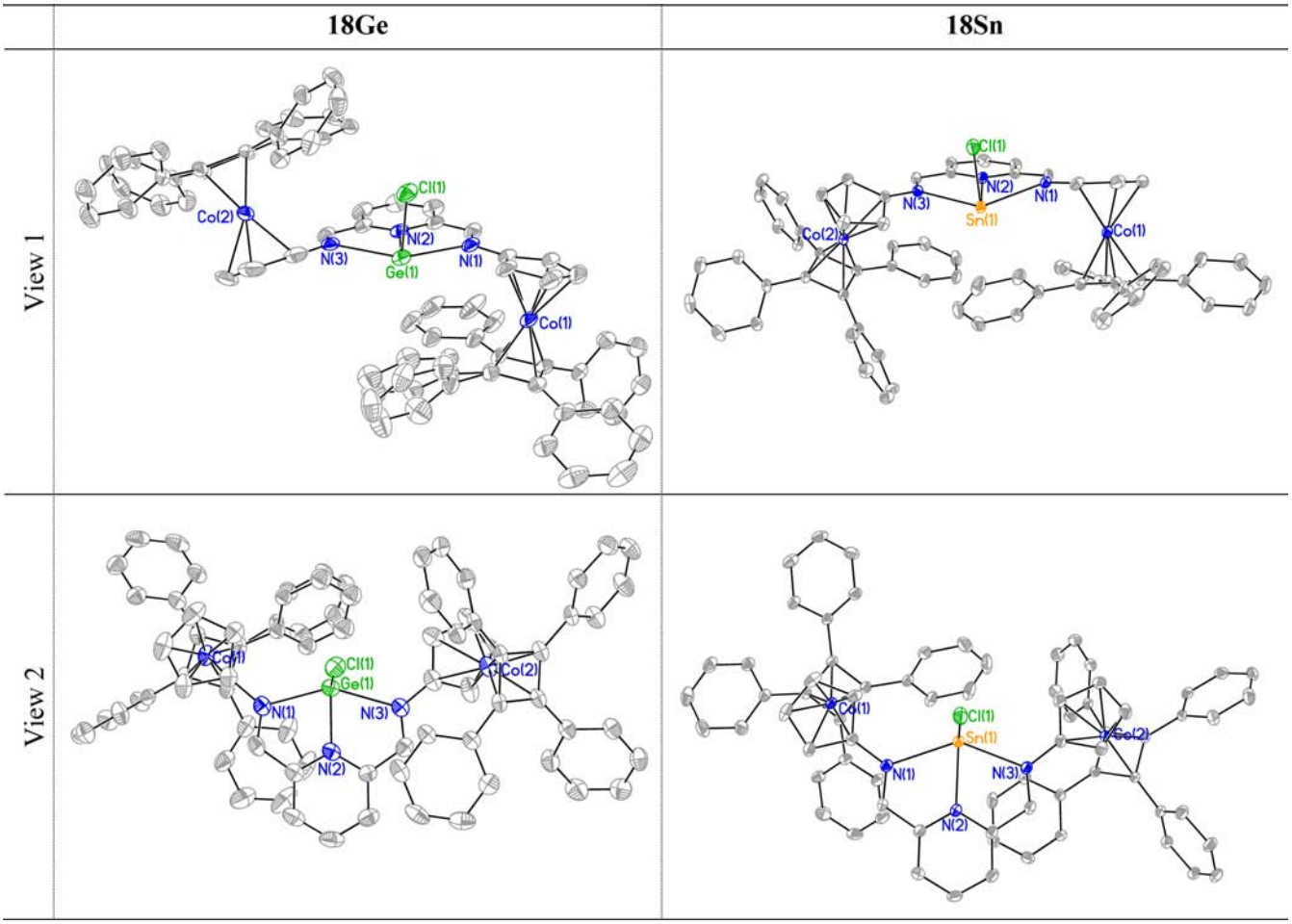

[a]Thermal ellipsoids are drawn to the 50% probability level. Solvates, anions, and hydrogen atoms are removed for clarity.

from this moiety under suitable structural and electrochemical conditions for the generation of a future novel redox active ligand.

EXPERIMENTAL SECTION

All manipulations were performed under an inert atmosphere in a nitrogen filled MBraun Labmaster dp glovebox or using standard Schlenk techniques unless stated otherwise. Reagents were obtained from commercial sources. All solvents were dried using an MBraun controlled atmospheres solvent purification system and stored in Straus flasks under a N_2 atmosphere or over 4 Å molecular sieves in the glovebox. Acetonitrile-d_3 and CD_2Cl_2 were purchased from Cambridge Isotope Laboratories and stored in the glovebox over 3 Å or 4 Å molecular sieves, respectively. The syntheses of **15**,[21] **17**,[20e] and 2,6-pyridinedialdehyde[24] were performed via literature procedures. Proton, $^{13}C\{^1H\}$, and $^{119}Sn\{^1H\}$ NMR spectroscopic data were collected on a 400 MHz Varian Inova spectrometer (399.762 MHz for ^1H; 100.52 MHz for ^{13}C; 149.163 MHz for ^{119}Sn). NMR spectra were recorded at room temperature, unless otherwise indicated, in CD_3CN or CD_2Cl_2 and were referenced using the residual protons of the deuterated solvents (CH_3CN, δ_H = 1.94; CH_2Cl_2, δ_H = 5.30); coupling constants are listed in hertz. Carbon-13 NMR spectra were referenced using carbon signals from the respective solvent (CH_3CN, δ_C = 1.32(7), 118.26(1); CH_2Cl_2, δ_C = 54.00(5)). Tin-119$\{^1H\}$ NMR spectra were recorded unlocked relative to an external standard ($^{119}Sn\{^1H\}$, Me_4Sn 90% in C_6D_6, δ_{Sn} = 0.00). Single crystal X-ray diffraction data were collected on a Nonius Kappa-CCD or a Bruker Apex II-CCD area detector using Mo Kα radiation (λ = 0.71073 Å). Crystals were selected under Paratone-N oil, mounted on MiTeGen micromounts or nylon loops, and then immediately placed in a cold stream of N_2. Structures were solved and refined using SHELXTL. UV/vis absorption spectra were recorded over a range of 235−800 nm using a Varian Cary 300 spectrometer in CH_2Cl_2. Compound **18Sn** was measured at a concentration of 1×10^{-5} M, while all other compounds had a concentration of 5×10^{-6} M. FT-IR spectra were collected on samples as KBr pellets using a Bruker Tensor 27 spectrometer, with a resolution of 4 cm^{-1}. Samples for FT-Raman spectroscopy were packed in capillary tubes and flame-sealed. Data were collected using a Bruker RFS 100/S spectrometer, with a resolution of 4 cm^{-1}. The dark composition of the solids made decomposition events difficult to assign by the traditional Gallenkamp variable heater method. Thermal degradation was instead determined using thermal gravimetric analysis (TGA) on a Q600 SDT TA Instruments: A sample of 5−15 mg was placed in an alumina cup and heated at a rate of 10 °C/min from room temperature to 800 °C under nitrogen atmosphere (100 mL/min). In all cases, two onsets of decomposition are reported, an initial temperature that occurs at mass losses between 2% and 10%, and then an additional decomposition that occurs with a much higher mass loss percentage. High resolution mass spectrometry (HRMS) was collected using a Finnigan MAT 8200 instrument. Elemental analyses (C, H, N) were performed by Laboratoire d'Analyze Élementaire de l'Université de Montreál, Montreál, QC, Canada. The electrochemical instrumentation employed for cyclic voltammetry (CV) was an Autolab30 electrochemical workstation equipped with GPES 4.9 software. The working electrode was either a glassy carbon (GC) disk electrode built from a GC rod (3 mm diameter) purchased from Tokai or 1 mm platinum disk working electrode as indicated. The disk electrode surface was

dx.doi.org/10.1021/ic401598e | Inorg. Chem. 2013, 52, 11311−11319

Table 3. Solid-State Structures of 15Ge and 15Sn[a]

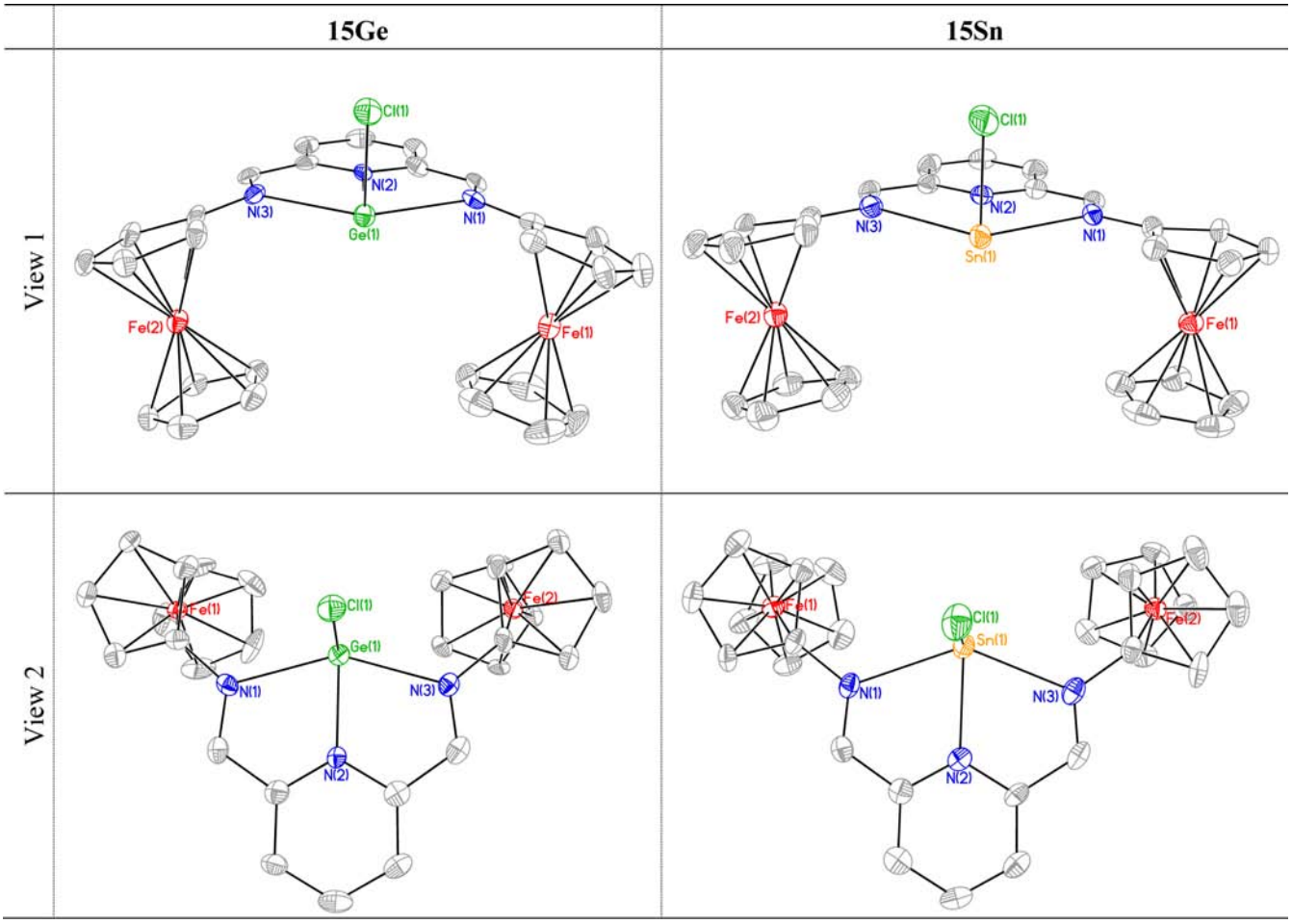

[a]Thermal ellipsoids are drawn to the 50% probability level. Solvates, anions, and hydrogen atoms are removed for clarity.

Table 4. X-Ray Details for Compounds 15Ge, 15Sn, 18Ge, and 18Sn

compound	15Ge	15Sn	18Ge	18Sn
empirical formula	$C_{27}H_{23}Cl_4Fe_2Ge_2N_3$	$C_{27}H_{23}Cl_4Fe_2N_3Sn_2$	$C_{77}H_{61}Cl_4Co_2Ge_2N_3O$	$C_{74}H_{55}Cl_6Co_2N_3Sn_2$
FW (g/mol)	788.16	880.36	1449.13	1554.25
crystal system	monoclinic	monoclinic	triclinic	triclinic
space group	$P2(1)/c$	$P2(1)/n$	$P\bar{1}$	$P\bar{1}$
a (Å)	12.791(7)	13.383(5)	10.980(5)	13.035(2)
b (Å)	28.663(16)	7.448(3)	14.830(7)	15.667(4)
c (Å)	7.870(4)	29.974(11)	22.891(10)	16.661(5)
α (deg)	90.00	90.00	107.17(2)	74.260(12)
β (deg)	104.54(1)	96.220(4)	91.04(1)	78.500(8)
γ (deg)	90.00	90.00	108.93(1)	77.023(15)
V (Å^3)	2793(3)	2970(2)	3342(3)	3156.5(13)
Z	4	4	2	2
D_c (mg m^{-3})	1.875	1.969	1.440	1.637
radiation, λ (Å)	0.71073	0.71073	0.71073	0.71073
temp (K)	110(2)	150(2)	150(2)	112(2)
$R1$ $[I > 2\sigma I]$[a]	0.0442	0.0380	0.0637	0.0494
$wR2$ (F^2)[a]	0.0982	0.0927	0.1523	0.1475
GOF (S)[a]	1.002	1.027	1.065	1.081

[a]$R1(F[I > 2(I)]) = \sum||F_o| - |F_c||/\sum|F_o|$; $wR2(F^2[\text{all data}]) = [w(F_o^2 - F_c^2)^2]^{1/2}$; $S(\text{all data}) = [w(F_o^2 - F_c^2)^2/(n - p)]^{1/2}$ (n = no. of data; p = no. of parameters varied; $w = 1/[^2(F_o^2) + (aP)^2 + bP]$ where $P = (F_o^2 + 2F_c^2)/3$ and a and b are constants suggested by the refinement program.

prepared by polishing on silicon carbide papers (500, 1200, 2400, and 4000) and successively over diamond pastes (1 and 0.25 μm) from Struers. The working electrode was stored in ethanol and, before using, was polished with diamond paste (1 μm), rinsed with dry ethanol, sonicated in dry ethanol for 5 min, and dried. This washing procedure was then repeated using 0.25 μm diamond paste to start.

dx.doi.org/10.1021/ic401598e | Inorg. Chem. 2013, 52, 11311−11319

Table 5. Selected Bond Lengths (Å) and Angles (deg) for 15Ge, 15Sn, 18Ge, and 18Sn and their analogues 16Ge and 16Sn

	15Ge	16Ge[22]	18Ge	15Sn	16Sn[22]	18Sn
M(1)−N(1)	2.271(4)	2.255(2)	2.297(4)	2.451(4)	2.403(2)	2.495(2)
M(1)−N(2)	2.052(4)	2.071(2)	2.064(4)	2.295(4)	2.286(2)	2.271(2)
M(1)−N(3)	2.251(4)	2.267(2)	2.316(4)	2.422(4)	2.411(2)	2.408(2)
C(1)−N(1)	1.294(6)	1.275(2)	1.275(6)	1.299(6)	1.274(3)	1.283(3)
C(7)−N(3)	1.284(6)	1.277(2)	1.276(6)	1.294(6)	1.280(3)	1.281(3)
M(2)−Cl(2)	2.2998(18)	2.3100(8)	2.258(2)	2.482(1)	2.4801(8)	2.4621(10)
M(2)−Cl(3)	2.3116(19)	2.3246(9)	2.330(2)	2.501(1)	2.5190(9)	2.446(6)
M(2)−Cl(4)	2.2911(17)	2.3128(9)	2.305(2)	2.522(1)	2.4870(8)	2.479(10)
N(1)−M(1)−Cl(1)	89.45(11)	87.18(5)	84.30(11)	86.50(10)	86.18(6)	86.62(5)
N(2)−M(1)−Cl(1)	96.50(13)	94.25(6)	94.68(11)	92.28(11)	88.31(6)	97.35(6)
N(3)−M(1)−Cl(1)	88.65(12)	88.09(5)	90.24(10)	85.53(10)	85.59(6)	83.56(6)
N(1)−M(1)−N(2)	73.59(16)	73.52(7)	73.78(15)	68.81(14)	68.71(7)	67.72(7)
N(2)−M(1)−N(3)	73.99(16)	73.28(7)	73.63(15)	68.82(14)	68.79(7)	69.17(7)
N(1)−M(1)−N(3)	147.08(16)	145.99(7)	146.35(14)	136.44(14)	136.87(7)	133.97(7)

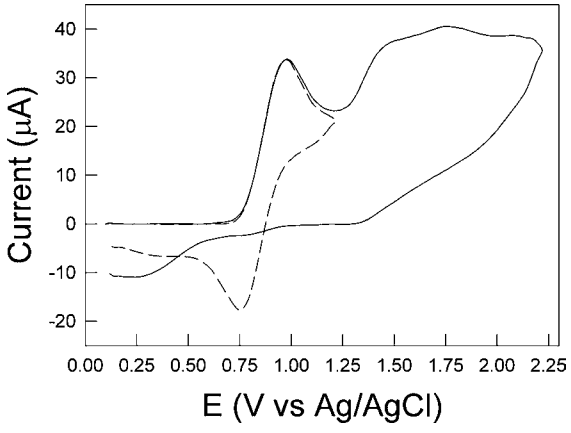

Figure 5. Cylic voltammograms of 2 mM solutions of **17** recorded at a Pt electrode in CH_2Cl_2/0.1 M $TBAPF_6$ at 5 V s^{-1}.

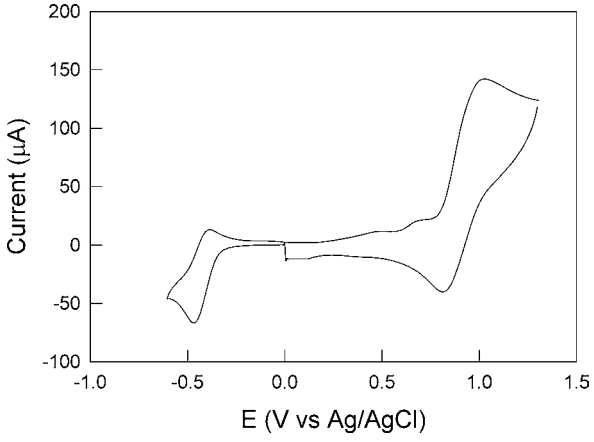

Figure 6. CV of **15Sn** recorded at a GC electrode in MeCN/0.1 M $TBAPF_6$ with analyte concentration 2 mM and at 0.5 V s^{-1}.

Electrochemical activation of the disk electrode surfaces was carried out before each measurement by multicycling between 0.0 and 0.5 V at 0.1 V s^{-1} in the background solution until stabilization of the capacitive current. The reference electrode was a stabilized Ag/AgCl quasi reference electrode, built by filling a glass tube closed at an extremity with a junction with an MeCN/0.1 M $TBAPF_6$ solution (or CH_2Cl_2/0.1 M $TBAPF_6$, matching the solvent used for the measurements). A silver wire was then immersed in the solution inside the glass tube, and the reference electrode was left to stabilize its potential for a week prior to use. At the end of every electrochemical

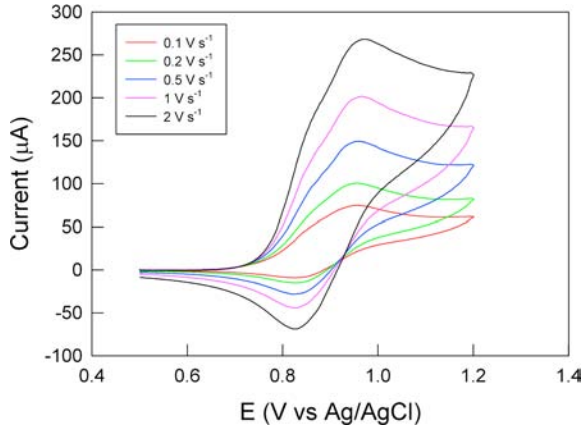

Figure 7. CV of **15Sn** recorded at different scan rates at a GC electrode in MeCN/0.1 M $P_{8888}TB$, and with analyte concentration 2 mM.

experiment, the CVs were calibrated using the reduction of nitrobenzene as an internal standard. In addition, the reversible reduction of nitrobenzene involves a single electron transfer; therefore the intensity of the voltammetric peak was used to gauge the number of electrons exchanged in the electrochemical processes of the studied compounds. The counter electrode was a platinum flag. Due to the sensitivity of the compounds to moisture and air, the experiments were performed inside of an MBraun Labmaster double station glovebox. The electrochemical characterization was performed using 2 mM analyte in 5 mL. For all measurements, feedback correction was employed to minimize the ohmic drop between reference and working electrode. The corresponding background curves were then subtracted from the CVs in order to eliminate the capacitive current contribution.

Synthesis: 18. Mixtures of **17** (0.152 g, 0.307 mmol) and 2,6-pyridinedialdehyde (0.021 g, 0.155 mmol) in 75 mL of THF were refluxed under an inert atmosphere for 1.5 h with constant stirring. The product precipitated out of solution during this time. The reaction mixture was then centrifuged, washed with THF (3 × 10 mL) and CH_2Cl_2 (3 × 10 mL), and dried *in vacuo* to give a fine light orange-red powder (0.135 g, 0.124 mmol, 80%). UV/vis (CH_2Cl_2): λ = 290 nm (40003 M^{-1} cm^{-1}), 319 nm (2990 M^{-1} cm^{-1}), 374 nm (20214 M^{-1} cm^{-1}), 441 nm (14121 M^{-1} cm^{-1}). FT-IR (cm^{-1} (ranked intensity)): 3056(13), 1616(1), 1601(5), 1583(6), 1534(12), 1498(10), 1460(2), 1368(14), 1344(8), 1278(7), 1241(3), 997(4), 692(15), 588(9), 101(11). FT-Raman (cm^{-1} (ranked intensity)): 3851(14), 3056(11), 1596(6), 1565(15), 1498(2), 1444(10), 1067(5), 1026(12), 815(9), 781(4), 700(1), 745(7), 589(8), 567(3), 544(13). Decomposition point: initial 131.5 °C (90.88%); final 378.41 °C (32.09%). HRMS $C_{73}H_{54}N_3Co_2$ calcd (found): 1090.29715 (1090.29763).

dx.doi.org/10.1021/ic401598e | *Inorg. Chem.* 2013, 52, 11311−11319

18Ge. A mixture of **18** (0.120 g, 0.110 mmol) in THF (3 mL) was added dropwise to a solution of $GeCl_2$·dioxane (0.051 g, 0.220 mmol) in THF (3 mL) at room temperature and was allowed to stir for 1 h. The solvent of the resulting dark green-black solution was then removed *in vacuo*. A minimal amount of CH_3CN was added to the solid, and Et_2O (3 × 10 mL) was added to precipitate out the product. Residual solvent was once again removed *in vacuo* to give a dark bluegreen-black powder (0.126 g, 0.091 mmol, 83%). Single crystals were obtained via vapor diffusion of CH_2Cl_2 into hexane. ^{1}H NMR (400 MHz, CD_2Cl_2, 25 °C, δ,): 8.64 (t, 1H, $^3J_{H-H}$ = 8.0), 7.80 (d, 2H, $^3J_{H-H}$ = 8.0), 7.56 (s, 2H), 7.33 (m, 16H), 7.18 (m, 8H), 7.12 (m, 16H), 5.33 (broad d, 4H), 5.10 (m, 4H). ^{13}C NMR (400 MHz, CD_2Cl_2, 25 °C, δ): 149.74, 146.93, 144.98, 134.42, 129.22, 128.81, 127.46, 104.99, 85.68, 80.10, 79.04, 69.05. UV/vis (CH_2Cl_2): λ = 289 nm (27859 M^{-1} cm^{-1}), 310 nm (21329 M^{-1} cm^{-1}), 414 nm (9271 M^{-1} cm^{-1}), 709 nm (5659 M^{-1} cm^{-1}). FT-IR (cm^{-1} (ranked intensity)): 1603(5), 1571(2), 1540(1), 1499(15), 1430(3), 1350(7), 1238(4), 1207(9), 1062(13), 1022(6), 999(10), 656(12), 588(8), 325(11), 219(14). FT-Raman (cm^{-1} (ranked intensity)): 3057(13), 1596(7), 1543(4), 1498(2), 1440(10), 1355(15), 1283(9), 1171(5), 1068(11), 808(14), 781(12), 739(6), 695(1), 587(8), 565(3). Decomposition point: initial 120.09 °C (98.60%); final 298.60 °C (32.09%). HRMS $C_{73}H_{53}Cl_1N_3Co_2Ge_1$ calcd (found): 1198.18359 (1198.18201).

18Sn. A mixture of **18** (0.080 g, 0.073 mmol) in THF (3 mL) was added dropwise to a solution of $SnCl_2$ (0.028 g, 0.147 mmol) in THF (3 mL) at room temperature and was stirred for 12 h. During this time, the orange slurry turned dark brown in color. The slurry was centrifuged, and the eluent was decanted into a vial, where the solvent was removed *in vacuo*. A minimal amount of CH_3CN was added to the solid, and Et_2O (3 × 5 mL) was added to precipitate out the product. Residual solvent was once again removed *in vacuo*, to give a dark blue-black powder (0.032 g, 0.022 mmol, 30%). Single crystals were obtained via vapor diffusion of CH_2Cl_2 into hexane. ^{1}H NMR (400 MHz, CD_2Cl_2, 25 °C, δ): 8.59 (t, 1H, $^3J_{H-H}$ = 8.0), 7.72 (d, 2H, $^3J_{H-H}$ = 8.0), 7.64 (s, 1H, $^3J_{Sn-H}$ = 32.0), 7.32 (m, 16H), 7.19 (m, 8H), 7.12 (m, 16H), 5.26 (m, 4H), 4.99 (m, 4H). ^{13}C NMR (400 MHz, CD_2Cl_2, 25 °C, δ): 199.30, 150.35, 144.73, 134.49, 130.45, 129.28, 128.88, 127.48, 105.92, 85.45, 78.92, 40.34. UV/vis (CH_2Cl_2): λ = 285 nm (25248 M^{-1} cm^{-1}), 310 nm (16648 M^{-1} cm^{-1}), 407 nm (6250 M^{-1} cm^{-1}), 694 nm (3646 M^{-1} cm^{-1}). FT-IR (cm^{-1} (ranked intensity)): 1600(3), 1569(4), 1538(1), 1498(15), 1432(2), 1352(8), 1235(5), 1203(7), 1057(14), 1017(6), 999(11), 655(13), 637(12), 588(9), 115(10). FT-Raman (cm^{-1} (ranked intensity)): 3851(15), 3455(14), 2961(11), 1595(9), 1538(7), 1497(4), 1437(13), 1280(12), 1262(6), 1024(2), 804(3), 740(8), 694(1), 587(10), 564(5). Decomposition point: initial 134.93 °C (98.49%); final 372.78 °C (15.89%). HRMS $C_{73}H_{53}Cl_1N_3Co_2Sn_1$ calcd (found): 1244.16225 (1244.16251).

15Ge. A solution of **15** (0.100 g, 0.200 mmol) in THF (3 mL) was added dropwise to a solution of $GeCl_2$ (0.092 g, 0.399 mmol) in CH_2Cl_2 (3 mL) at room temperature and was allowed to stir for 30 min. The product was precipitated by the addition of *n*-pentane (3 × 10 mL) and Et_2O (3 × 10 mL) and dried *in vacuo* to give a fine dark lustrous green solid (0.71 g, 0.090 mmol, 45%). Single crystals were obtained via vapor diffusion of CH_2Cl_2 into hexane. ^{1}H NMR (600 MHz, CD_3CN, 25 °C, δ): 9.13 (s, 2H), 8.56 (t, 1H, $^3J_{H-H}$ = 6.0), 8.21 (d, 2H, $^3J_{H-H}$ = 6.0), 5.21 (m, 2H), 4.83 (m, 2H), 4.39 (s, 10H). UV/vis (CH_2Cl_2): λ = 263 nm (26895 M^{-1} cm^{-1}), 337 nm (23670 M^{-1} cm^{-1}), 381 nm (21523 M^{-1} cm^{-1}), 439 nm (14552 M^{-1} cm^{-1}), 739 nm (10595 M^{-1} cm^{-1}). FT-IR (cm^{-1} (ranked intensity)): 3094(14), 1604(5), 1570(10), 1537(1), 1481(11), 1428(2), 1284(3), 1236(12), 1168(6), 1108(9), 1039(8), 935(7), 822(13), 801(2), 541(15), 504(4). FT-Raman (cm^{-1} (ranked intensity)): 1601(9), 1588(15), 1569(2), 1535(1), 1427(3), 1235(4), 1204(8), 1059(12), 1020(6), 656(10), 639(5), 591(11), 487(14), 307(7), 85(13). Decomposition point: initial 241.92 °C (95.35%); final 370.07 °C (66.26%). HRMS $C_{27}H_{23}Cl_1N_3Fe_2Ge_1$ calcd (found): 609.9500 (609.9494). Elemental anal. calcd for $C_{27}H_{23}Cl_4N_3Fe_2Ge_2$: 41.14% C, 2.94% H, 5.33% N. Found: 41.68% C, 2.81% H, 5.31% N.

15Sn. A solution of **15** (0.085 g, 0.170 mmol) in THF (3 mL) was added dropwise to a solution of $GeCl_2$ (0.064 g, 0.339 mmol) in THF (3 mL) at room temperature and was allowed to stir for 30 min. The product was precipitated by the addition of *n*-pentane, centrifuged, washed with additional *n*-pentane (3 × 10 mL), and finally dried *in vacuo* to give a fine dark lustrous blue solid (0.094 g, 0.107 mmol, 63%). Single crystals were obtained via vapor diffusion of CH_2Cl_2 into hexane. ^{1}H NMR (600 MHz, CD_3CN, 25 °C, δ): 9.18 (s, 2H, $^3J_{Sn-H}$ = 36.0), 8.52 (t, 1H, $^3J_{H-H}$ = 6.0), 8.17 (d, 2H, $^3J_{H-H}$ = 6.0), 5.13 (broad s, 4H), 4.79 (m, 4H), 4.42 (s, 10H). ^{13}C NMR (400 MHz, CD_3CN, 25 °C, δ): 152.16, 151.69, 146.03, 129.86, 72.52, 72.22, 69.99, 37.46. ^{119}Sn{^{1}H} NMR (400 MHz, CD_3CN, 25 °C, δ): 262.56, 482.42. UV/vis (CH_2Cl_2): λ = 255 nm (27164 M^{-1} cm^{-1}), 337 nm (19236 M^{-1} cm^{-1}), 430 nm (12087 M^{-1} cm^{-1}), 692 nm (8846 M^{-1} cm^{-1}). FT-IR (cm^{-1} (ranked intensity)): 3090(13), 1603(5), 1544(1), 1475(11), 1432(6), 1365(15), 1282(4), 1168(8), 1107(9), 1036(7), 1002(14), 937(10), 805(3), 539(12), 499(2). FT-Raman (cm^{-1} (ranked intensity): 3098(10), 1601(4), 1574(3), 1544(1), 1433(2), 1236(5), 1217(12), 1201(8), 1059(13), 1019(6), 659(11), 640(7), 592(14), 305(9). Decomposition point: initial 222.78 °C (98.19%); final 447.58 °C (73.80%). HRMS $C_{27}H_{23}Cl_1N_3Fe_2Sn_1$ calcd (found): 655.92903 (655.93014).

■ ASSOCIATED CONTENT

Ⓢ Supporting Information

^{1}H NMR spectra for **15**, **15Ge**, and **15Sn**, ^{119}Sn NMR spectrum of **15Sn**, UV-vis spectra for compounds **18**, **18Ge**, **18Sn**, **15Ge**, and **15Sn**, structure diagrams showing disorder in **18Ge** and **18Sn**, photograph of solutions of **18** (CH_2Cl_2), **18Ge** (CH_2Cl_2), **18Sn** (CH_2Cl_2), **15** (CH_2Cl_2), **15Ge** (MeCN), and **15Sn** (MeCN), and crystallographic information for **18Ge**, **18Sn**, **15Ge**, and **15Sn** in CIF format. This material is available free of charge via the Internet at http://pubs.acs.org.

■ AUTHOR INFORMATION

Corresponding Author

*E-mail: pragogna@uwo.ca.

Notes

The authors declare no competing financial interest.

■ ACKNOWLEDGMENTS

The authors are very grateful to the Natural Sciences and Engineering Research Council of Canada (NSERC), the Canada Foundation for Innovation, Ontario Ministry of Research and Innovation, and Western University for generous financial support. We also thank J. W. Dube for his assistance with the X-ray crystallographic studies.

■ REFERENCES

(1) Luca, O. R.; Crabtree, R. H. *Chem. Soc.Rev.* **2013**, *42*, 1440.
(2) Chirik, P. J. *Inorg. Chem.* **2011**, *50*, 971.
(3) Chirik, P. J.; Wieghardt, K. *Science* **2010**, *327*, 794.
(4) Kaim, W.; Schwederski, B. *Coord. Chem. Rev.* **2010**, *254*, 1580.
(5) Praneeth, V. K. K.; Ringenberg, M. R.; Ward, T. R. *Angew. Chem., Int. Ed.* **2012**, *51*, 10228.
(6) Allgeier, A. M.; Mirkin, C. A. *Angew. Chem., Int. Ed.* **1998**, *37*, 894.
(7) Purse, B. W.; Tran, L. H.; Piera, J.; Åkermark, B.; Bäckvall, J.-E. *Chem.—Eur. J.* **2008**, *47*, 3506.
(8) Tennyson, A. G.; Lynch, V. M.; Bielawski, C. W. *J. Am. Chem. Soc.* **2010**, *132*, 9420.
(9) Saravanakumar, S.; Kindermann, M. K.; Heinicke, J.; Kockerling, M. *Chem. Commun.* **2006**, 640–642.
(10) McSkimming, A.; Bhadhade, M.; Colbran, S. B. *Dalton Trans.* **2010**, *39*, 10581.

(11) McSkimming, A.; Ball, G. E.; Bhadhade, M. M.; Colbran, S. B. *Inorg. Chem.* **2012**, *51*, 2191.
(12) Gregson, C. K. A.; Gibson, V. C.; Long, N. J.; Marshall, E. L.; Oxford, P. J.; White, A. J. P. *J. Am. Chem. Soc.* **2006**, *128*, 7410−7411.
(13) Gibson, V. C.; Long, N. J.; Oxford, P. J.; White, A. J. P.; Williams, D. J. *Organometallics* **2006**, *25*, 1932−1939.
(14) Bildstein, B.; Malaun, M.; Kopacka, H.; Fontani, M.; Zanello, P. *Inorg. Chim. Acta* **2000**, *300*−*302*, 16−22.
(15) Multani, K.; Stanlake, L. J. E.; Stephan, D. W. *Dalton Trans.* **2010**, *39*, 8957−8966.
(16) Stanlake, L. J. E.; Stephan, D. W. *Dalton Trans.* **2011**, *40*, 5836−5840.
(17) Plenio, H.; Burth, D. *Organometallics* **1996**, *15*, 4054.
(18) Lorković, I. M.; Wrighton, M. S.; Davis, W. M. *J. Am. Chem. Soc.* **1994**, *116*, 6220−6228.
(19) Lorkovic, I. M.; Duff, R. R., Jr.; Wrighton, M. S. *J. Am. Chem. Soc.* **1995**, *117*, 3617−3618.
(20) (a) Cassar, D. J.; Nagaradja, E.; Butler, D. C. D.; Villemin, D.; Richards, C. J. *Org. Lett.* **2012**, *14*, 894−897. (b) Gunay, M. E.; Hughes, D. L.; Richards, C. J. *Organometallics* **2011**, *30*, 3901−3904. (c) Anderson, C. E.; Overman, L. E.; Richards, C. J.; Watson, M. P.; N. White, N. *Org. Synth.* **2007**, *84*, 139. (d) Roca, F. X.; Motevalli, M.; Richards, C. J. *J. Am. Chem. Soc.* **2005**, *127*, 2388. (e) Butler, D. C. D.; Richards, C. J. *Organometallics* **2002**, *21*, 5433−5436. (f) Stevens, A. M.; Richards, C. J. *Organometallics* **1999**, *18*, 1346.
(21) Magdzinski, E.; Gobbo, P.; Martin, C. D.; Workentin, M. S.; Ragogna, P. J. *Inorg. Chem.* **2012**, *51*, 8425.
(22) Singh, A. P.; Roesky, H. W.; Carl, E.; Stalke, D.; Demers, J.-P.; Lange, A. *J. Am. Chem. Soc.* **2012**, *134*, 4998.
(23) duMont, W. W.; Kroth, H. J. *Z. Naturforsch. B* **1980**, *35b*, 700.
(24) Jerchel, D.; Heck, H. E. *Liebigs Ann. Chem.* **1958**, *613*, 180.